International Journal of Control

ISSN: 0020-7179 (Print) 1366-5820 (Online) Journal homepage: https://www.tandfonline.com/loi/tcon20

Model reduction of parabolic PDEs using multivariate splines

H. J. Tol, C. C. de Visser & M. Kotsonis

To cite this article: H. J. Tol, C. C. de Visser & M. Kotsonis (2019) Model reduction of parabolic PDEs using multivariate splines, International Journal of Control, 92:1, 175-190, DOI: 10.1080/00207179.2016.1222554

To link to this article: https://doi.org/10.1080/00207179.2016.1222554

INTERNATIONAL JOURNAL OF CONTROL
2019, VOL. 92, NO. 1, 175–190
http://dx.doi.org/10.1080/00207179.2016.1222554

Taylor & Francis
Taylor & Francis Group

Model reduction of parabolic PDEs using multivariate splines

H. J. Tol, C. C. de Visser and M. Kotsonis

Delft University of Technology, Faculty of Aerospace Engineering, The Netherlands

ABSTRACT

A new methodology is presented for model reduction of linear parabolic partial differential equations (PDEs) on general geometries using multivariate splines on triangulations. State-space descriptions are derived that can be used for control design. This method uses Galerkin projection with B-splines to derive a finite set of ordinary differential equations (ODEs). Any desired smoothness conditions between elements as well as the boundary conditions are flexibly imposed as a system of side constraints on the set of ODEs. Projection of the set of ODEs on the null space of the system of side constraints naturally produces a reduced-order model that satisfies these constraints. This method can be applied for both in-domain control and boundary control of parabolic PDEs with spatially varying coefficients on general geometries. The reduction method is applied to design and implement feedback controllers for stabilisation of a 1-D unstable heat equation and a more challenging 2-D reaction–convection–diffusion equation on an irregular domain. It is shown that effective feedback stabilisation can be achieved using low-order control models.

ARTICLE HISTORY
Received 17 November 2015
Accepted 6 August 2016

KEYWORDS
Distributed parameter systems; multivariate splines; Galerkin's method; parabolic partial differential equations

1. Introduction

This paper presents a reduced-order modelling approach for control of distributed parameter systems (DPS) on general geometries using multivariate B-splines defined on triangulations (de Boor, 1987; Farin, 1986; Lai & Schumaker, 2007). With DPS the system state, input, output and parameters vary both spatially and temporally. This paper focuses on DPS governed by parabolic partial differential equations (PDEs) which, for example, arise in the context of chemical processes, thermal processes and fluid dynamic systems. PDE control theory often focuses on extending finite-dimensional results such as stability and optimal control to the infinite-dimensional case (see Curtain and Zwart (1995) and Lasiecka and Triggiani (2000) for a more complete coverage, and references therein). While mathematically precise, these results are often derived for general classes of PDEs, and for systems defined on 2-D/3-D general geometries, only abstract results are typically available.

This led to the attention of structure-specific opportunities that exist in PDEs to produce results that are both constructive and mathematically rigorous (Bamieh, Paganini, & Dahleh, 2002; Smyshlyaev & Krstic, 2004). Constructive methods for solving optimal control problems for a class of spatially invariant systems with distributed sensing and actuation was first presented in Bamieh et al. (2002). By applying a Fourier transform to the system along the spatially invariant coordinates, the system can be block-diagonalised and decoupled in terms of a frequency parameter that replaces the spatially invariant coordinate (Bamieh et al., 2002). In this way, analysis and design of the controller can be carried out on a parameterised lower dimensional system and later reconstructed in the physical space (Bamieh et al., 2002; Hagen, Mezić, & Bamieh, 2004). In Smyshlyaev and Krstic (2004, 2005), a closed-form continuous backstepping control/observer design method was first presented for stabilisation of a class of 1-D parabolic PDEs. The backstepping method has the powerful feature that it produces explicitly computable gains and has been extended to higher dimensional spatial domains and systems of coupled PDEs. We refer to Baccoli, Pisano, and Orlov (2015) for a recent overview of developments of the backstepping method. In particular, by also exploiting spatial invariance, this method has led to explicit solutions for 2-D and 3-D spatially invariant control problems (Vazquez & Krstic, 2007b) such as the Navier–Stokes channel flow (Vazquez & Krstic, 2007a).

Many practical engineering problems are formulated in spatially variant geometries such as irregular channels or require that the controls and sensors are spatially localised. In this case, a finite-dimensional approximation of the infinite-dimensional system is often required. Model reduction is the process of reducing the infinite-dimensional PDE to a finite set of ODEs that can be used for control design. We refer to Li and Qi (2010)

CONTACT H. J. Tol h.j.tol@tudelft.nl

for a recent review on model reduction techniques for PDEs. Galerkin projection is most commonly applied to parabolic PDEs and in this method, one obtains a lower dimensional approximation by projecting the PDE onto a set of spatial basis functions that contain characteristics of the expected solution. The orthogonality of the projection ensures the best possible solution in the space spanned by the basis functions. The main advantage of this approach is that it is robust with respect to the truncated dynamics; a controller which exponentially stabilises the closed-loop ODE system also stabilises the closed-loop parabolic PDE system (Balas, 1979, 1983, 1984). On the other hand, it may require a large number of modes to derive an ODE system with the desired degree of accuracy. Selection of the spatial basis functions is critical and has a great impact to the modelling performance.

A feature of most parabolic PDE systems is that the eigenspectrum of the spatial differential operator shows a clear separation between a finite-dimensional slow part and an infinite-dimensional fast complement (Balas, 1979). If the eigenfunctions of the spatial differential operator are known, a suitable choice for model reduction is, therefore, the projection of the system on the modal subspace spanned by the dominant eigenfunctions (Armaou & Christofides, 2001; Christofides, 2001; Christofides & Baker, 1999). This requires analytic solutions of the spatial differential operator eigenvalue problem to form the modal subspace which are often not available for systems defined on irregular domains and systems with spatially varying coefficients. Another approach is to utilise simulation data or experimental data of the PDE system to compute a set of empirical eigenfunctions through the proper orthogonal decomposition (POD) method (see e.g. Armaou & Christofides, 2001, 2002; Baker, Armao, & Christofides, 2000). The POD method is a statistical technique that extracts the most energetic modes from a set of snapshots and therefore leads to low-order expansions. The POD method is applicable to a wide range of DPS, including those defined on irregular domains. However, each set of POD modes is intrinsic to a particular simulation or snapshots and its effectiveness is highly dependent on the simulation/experimental settings (Li & Qi, 2010; Rowley, 2005). It also has limitations for the describing input–output behaviour of the system (Rowley, 2005).

This paper introduces a new systematic approach for model reduction of parabolic PDEs on general geometries using multivariate B-splines defined on triangulations (de Boor, 1987; Farin, 1986; Lai & Schumaker, 2007). This method uses Galerkin projection with B-splines to derive a finite set of ODEs. The multivariate B-spline consists of piecewise-defined polynomials of arbitrary degree called B-form polynomials. Any desired smoothness conditions between elements as well as the boundary conditions are flexibly imposed as a system of side constraints on the set of ODEs. Projection of the set of ODEs on the null space of the system of side constraints naturally produces a reduced-order model that satisfies these constraints. The multivariate B-spline has been used in the past to find numerical solutions for elliptic PDEs (Awanou, Lai, & Wenston, 2005; Hu, Han, & Lai, 2007) and steady Navier–Stokes equations (Awanou & Lai, 2004; Lai & Wenston, 2004) based on energy methods, and to find numerical solutions for Hamilton–Jacobi–Bellman PDEs using the collocation method (Govindarajan, de Visser, & Krishnakumar, 2014). This work is different in the sense that it is does not find explicit numerical solutions for PDEs. Instead, the PDE is spatially discretised and converted to a linear state-space representation that is used for control design.

The main contribution of the paper is a new framework to derive state-space descriptions for a class of parabolic PDEs to which standard control theoretic tools can be applied. The main advantage of this method is that it is general in the sense that it can be applied for both in-domain control and boundary control of parabolic PDEs with spatially varying coefficients defined on general geometries. It is in particular useful for parabolic PDEs for which analytic solutions of the spatial differential operator eigenvalue problem are not possible. We are also able to use multivariate spline functions of variable degrees and variable smoothness across any given domain. These properties make spline functions more user-friendly compared to standard finite elements. Splines with higher order smoothness can directly be implemented to approximate the strong solution of the PDE system and polynomials of high degrees can be easily used to get better approximation properties (Awanou et al., 2005; Awanou & Lai, 2004; Hu et al., 2007). The degree and order of continuity of splines are simply input variables for creating the state-space models which can also be tuned to achieve a desirable trade-off between the accuracy and the order of the model. Together with the mesh flexibility, this method allows the construction of reduced-order models which are both accurate and suitable for online applications. We refer to Awanou et al. (2005) for an overview of more features of multivariate splines and references within. Compared to POD–Galerkin methods, this approach may lead to higher order models, but in return provides a systematic approach in which the input–output behaviour of the system is easily established. This method can also be used in conjunction with other open-loop truncation methods for state-space systems such as balanced POD (Rowley, 2005) and balanced truncation. This

combination can open a new route towards the control of more complex problems such as the three-dimensional Navier–Stokes equations.

In this paper, we restrict our attention to a linear class of parabolic PDEs. Nonlinear parabolic PDEs are also tractable for the spline Galerkin method and, in the most general case, lead to nonlinear state space descriptions of the PDE. To accurately capture the nonlinear couplings between the fast and slow modes without using a high-order model, the Galerkin method should be used in combination with (approximate) inertial manifolds to compensate the fast modes with the slow modes (Armaou & Christofides, 2001; Baker et al., 2000; Christofides & Daoutidis, 1997). Nonlinear model reduction and control of parabolic PDEs will, therefore, be considered in a forthcoming study.

The outline of the paper is as follows. In Section 2, the class of parabolic PDEs and control types for which the reduction method can be applied is formulated. In Section 3, a preliminary on multivariate B-splines is given. In Section 4, the side constraints for the boundary conditions are derived using new expressions for differential operators acting on B-splines. Section 5 contains the main contribution of this paper in which the state-space descriptions are derived, and in Section 6, the state-space models are used to synthesise the output feedback controller. Finally, in Section 7, the reduction method is used to implement the feedback controllers for stabilisation of a 1-D unstable heat equation and a 2-D unstable reaction–convection–diffusion equation on an irregular domain, followed by conclusions in Section 8.

2. Class of systems under consideration

Let Ω be an open-bounded subset of $\mathbb{R}^n$ with a Lipschitz-continuous boundary Γ and set $\Omega_T = \Omega \times (0, T]$ for some fixed time $T > 0$. In this paper, we consider linear parabolic PDEs, with the following state space description:

$$\frac{\partial y(x,t)}{\partial t} = Ly(x,t) + g(x)u(t) \quad \text{in } \Omega_T \tag{1a}$$

$$L_\Gamma y(x,t) = g_\Gamma(x)u_\Gamma(t) \quad \text{on } \Gamma_T \tag{1b}$$

$$z_{m_k}(t) = \int_\Omega \delta(x - x_k) L_{z_m} y(x,t), \quad k = 1, \cdots, K \tag{1c}$$

$$z_{c_i}(t) = \int_\Omega \phi_i(x) L_{z_c} y(x,t) dx, \quad i = 1, \cdots, Q \tag{1d}$$

with $y(x,t)$ the state variable, $x \in \Omega$ the spatial coordinate, $z_{m_k} \in \mathbb{R}$ a measured output and $z_{c_i} \in \mathbb{R}$ a controlled output which is used to define the control objective later in this section. The vector function $g(x) = [g_1(x), \ldots, g_m(x)]$, $g_i \in \mathcal{L}^2(\Omega)$ describes how the inputs $u(t) = [u_1(t), \ldots, u_m(t)]^T \in \mathbb{R}^m$ from m linear actuators are distributed in the domain, $g_\Gamma(x) = [g_{\Gamma,1}(x), \ldots, g_{\Gamma,m}(x)]$, $g_{\Gamma,i} \in \mathcal{L}^2(\Gamma)$ describes how the inputs $u_\Gamma(t) = [u_{\Gamma,1}(t), \ldots, u_{\Gamma,m}(t)]^T \in \mathbb{R}^{m_\Gamma}$ are distributed over the boundary and $\phi_i(x)$ is determined by the desired performance specifications in the domain Ω. The operator L is defined as a linear partial differential operator with derivatives up to order $k \geq 1$ with spatially varying coefficients

$$L = \sum_{|\alpha| \leq k} a_\alpha(x) D^\alpha = a_0(x) + \sum_{1 \leq |\alpha| \leq k} a_\alpha(x) D^\alpha \tag{2}$$

where we have used the well-known multi-index notation for the spatial derivative

$$D^\alpha y = \frac{\partial^{|\alpha|} y}{\partial x_1^{\alpha_1} \partial x_2^{\alpha_2} \cdots \partial x_n^{\alpha_n}} \tag{3}$$

for a given multi-index $(\alpha_1, \alpha_2, \ldots, \alpha_n)$ of order $|\alpha| = \alpha_1 + \alpha_2 + \cdots + \alpha_n$ and the operators $L_\Gamma, L_{z_c}, L_{z_m}$ are defined as partial differential operators with constant coefficients. Common boundary conditions are Dirichlet ($L_\Gamma = I$), Neumann ($L_\Gamma = \frac{\partial}{\partial n}$) and Robin boundary conditions ($L_\Gamma = I + \frac{\partial}{\partial n}$). In this study, feedback stabilisation of (1a) is considered where the PDE describes the error between the unsteady response and the equilibrium profile, e.g. the error between the unsteady temperature and the equilibrium profile of the temperature. It is assumed that point measurements from K boundary or in-domain sensors are used for feedback.

The objective is to reduce the infinite-dimensional state-space system (1) to a finite-dimensional state-space system using multivariate splines, which can be used to synthesise any suitable linear controller. In this study, a classical linear quadratic optimal control problem is considered. To define the control objective, the system (1) is formulated as an infinite-dimensional system in a Hilbert space (Christofides & Daoutidis, 1997; Curtain & Zwart, 1995). The derivation of this system is also closely related to the derivation of the reduced-order model in Section 5. Let $\mathcal{H}$ be the space of functions defined on Ω that satisfy the boundary conditions (1b), with inner product $(y_1, y_2) = \int_\Omega y_1 y_2 dx$ and norm $\|y_1\|_2 = (y_1, y_1)^{1/2}$ where $y_1, y_2 \in \mathcal{H}$. Furthermore, let the trajectory segment $y(\cdot, t) = \{y(x,t), x \in \Omega\}$ be the state and $y(t)|_\Gamma \in \mathcal{U}$ the value of $y(t)$ on the boundary defined in a separable Hilbert space $\mathcal{U}$. Defining the following operators on

$\mathcal{H}$ as

$$\begin{aligned}
&\mathfrak{A} : D(\mathfrak{A}) \subset \mathcal{H} \mapsto \mathcal{H}, \qquad \mathfrak{A}y(t) = Ly(t)\\
&\mathcal{A}_\Gamma : D(\mathcal{A}_\Gamma) \subset \mathcal{H} \mapsto \mathcal{U}, \quad \mathcal{A}_\Gamma y(t) = L_\Gamma y(t)|_\Gamma\\
&\mathcal{A} : D(\mathcal{A}) \mapsto \mathcal{H}, \quad \mathcal{A}y(t) = \mathfrak{A}y(t), \text{ for } y \in D(\mathcal{A}),\\
&D(\mathcal{A}) = D(\mathfrak{A}) \cap ker(\mathcal{A}_\Gamma) = \left\{y \in \mathcal{H}; L_\Gamma y(t)|_\Gamma = 0\right\}
\end{aligned} \tag{4}$$

where $D(\mathcal{A})$ denotes the domain of $\mathcal{A}$, defining the input and output operators as

$$\begin{aligned}
&\mathcal{B} : \mathbb{R}^m \mapsto \mathcal{H}, \qquad \mathcal{B}u(t) = g(x)u(t)\\
&\mathcal{B}_\Gamma : \mathbb{R}^{m_\Gamma} \mapsto \mathcal{U}, \quad \mathcal{B}_\Gamma u_\Gamma(t) = g_\Gamma(x)u_\Gamma(t)\\
&\mathcal{C}_{m_k} : \mathcal{H} \mapsto \mathbb{R}, \quad \mathcal{C}_{m_k} y(t) = \left(\delta(x - x_k), L_{z_m} y(t)\right)\\
&\mathcal{C}_{c_i} : \mathcal{H} \mapsto \mathbb{R}, \quad \mathcal{C}_{c_i} y(t) = \left(\phi_i(x), L_{z_c} y(t)\right)
\end{aligned} \tag{5}$$

construct an operator $\mathcal{Q}$ such that

$$\mathcal{Q} : \mathcal{U} \mapsto \mathcal{H}, \quad \mathcal{A}_\Gamma \mathcal{Q}\mathcal{B}_\Gamma u_\Gamma(t) = \mathcal{B}_\Gamma u_\Gamma(t) \tag{6}$$

system (1) can be formulated as (Curtain & Zwart, 1995)

$$\begin{aligned}
\frac{\partial \tilde{y}(t)}{\partial t} &= \mathcal{A}\tilde{y}(t) - \mathcal{Q}\mathcal{B}_\Gamma \dot{u}_\Gamma(t) + \mathfrak{A}\mathcal{Q}\mathcal{B}_\Gamma u_\Gamma(t)\\
&\quad + \mathcal{B}u(t), \quad \tilde{y}(0) = \tilde{y}_0\\
z_m(t) &= \mathcal{C}_m(\tilde{y}(t) + \mathcal{Q}\mathcal{B}_\Gamma u_\Gamma(t))\\
z_c(t) &= \mathcal{C}_c(\tilde{y}(t) + \mathcal{Q}\mathcal{B}_\Gamma u_\Gamma(t))
\end{aligned} \tag{7}$$

where the solution of (7) is related to the classical solution of (1) by

$$y(t) = \tilde{y}(t) + \mathcal{Q}\mathcal{B}_\Gamma u_\Gamma(t). \tag{8}$$

From (6) and (8), it follows that $\tilde{y}(t)$ can be regarded as a homogeneous solution and $\mathcal{Q}\mathcal{B}_\Gamma u_\Gamma(t)$ as a particular solution that satisfies the boundary conditions. Equation (7) can also be formulated in the infinite-dimensional state space format

$$\begin{aligned}
\dot{x}(t) &= \bar{\mathcal{A}}x(t) + \bar{\mathcal{B}}\bar{u}(t), \quad x(0) = x_0\\
z_m(t) &= \bar{\mathcal{C}}_m x(t), \quad z_c(t) = \bar{\mathcal{C}}_c x(t)
\end{aligned} \tag{9}$$

where

$$\begin{aligned}
&x(t) = \begin{bmatrix}\tilde{y}^T(t) & u_\Gamma^T(t)\end{bmatrix}^T, \quad \bar{u}(t) = \begin{bmatrix}u^T(t) & \dot{u}_\Gamma^T(t)\end{bmatrix}^T\\
&\bar{\mathcal{A}} = \begin{bmatrix}\mathcal{A} & \mathfrak{A}\mathcal{Q}\mathcal{B}_\Gamma\\ 0 & 0\end{bmatrix}, \quad \bar{\mathcal{B}} = \begin{bmatrix}\mathcal{B} & -\mathcal{Q}\mathcal{B}_\Gamma\\ 0 & I\end{bmatrix}\\
&\bar{\mathcal{C}}_m = \begin{bmatrix}\mathcal{C}_m & \mathcal{C}_m\mathcal{Q}\mathcal{B}_\Gamma\end{bmatrix}, \quad \bar{\mathcal{C}}_c = \begin{bmatrix}\mathcal{C}_c & \mathcal{C}_c\mathcal{Q}\mathcal{B}_\Gamma\end{bmatrix}
\end{aligned} \tag{10}$$

The control objective is to synthesise an output feedback that minimises the quadratic (LQR) cost function

$$\mathcal{J} = \int_0^\infty (z_c, z_c)_{\mathbb{R}^n} + (\bar{u}, R\bar{u})_{\mathbb{R}^n}\, dt \tag{11}$$

where $(\cdot,\cdot)_{\mathbb{R}^n}$ denotes the standard inner product in $\mathbb{R}^n$.

3. Preliminaries on multivariate splines

Given a bounded polygonal domain $\Omega \in \mathbb{R}^n$ and let $\mathcal{T}$ be a triangulation of Ω. The spline space is the space of all smooth piecewise polynomial functions of degree d and smoothness r over $\mathcal{T}$ with $0 \le r < d$

$$S_d^r(\mathcal{T}) := s \in C^r(\Omega) : s|_\Delta \in \mathcal{P}_d, \forall \Delta \in \mathcal{T} \tag{12}$$

where $\mathcal{P}_d$ denotes the space of all polynomials of total degree d and Δ denotes an n-simplex (line in 1-D, triangle in 2-D, tetrahedron in 3-D) and $\Omega = \bigcup_{\Delta\in\mathcal{T}} \Delta$. In this paper, the B-form representation of splines defined on triangulations is used (de Boor, 1987; Farin, 1986). Only the essential theory that is necessary for the treatment of the spline model reduction framework is discussed here. We refer to Lai and Schumaker (2007) for a more complete coverage.

Let $\Delta = \langle v_0, v_1, \ldots, v_n\rangle$ be an n-simplex with vertices $v_i = (x_1^{(i)}, x_2^{(i)}, \ldots, x_n^{(i)})$. A separate local coordinate system can be defined for each simplex in terms of barycentric weights. In this coordinate system, every point $x = (x_1, x_2, \ldots, x_n) \in \mathbb{R}^n$ is described in terms of a unique weighted vector sum of the vertices of Δ

$$x = \sum_{i=0}^n b_i v_i, \quad \sum_{i=0}^n b_i = 1 \tag{13}$$

where $b = (b_0, b_1, \ldots, b_n) \in \mathbb{R}^{n+1}$ is called the barycentric coordinate of point $x = (x_1, \ldots, x_n)$ relative to simplex Δ. In the remainder of this paper, we denote $b_{\Delta_j}(x) : \mathbb{R}^n \to \mathbb{R}^{n+1}$ as the mapping from Cartesian coordinates to barycentric coordinates for a specific simplex with $b = b_{\Delta_j}(x)$.

The simplex polynomials are expressed in terms of Bernstein–Bézier basis polynomials of degree d

$$B_\kappa^d(b_{\Delta_j}(x)) = \begin{cases} \dfrac{d!}{\kappa_0!\kappa_1!\cdots\kappa_n!} b_0^{\kappa_0} b_1^{\kappa_1} \cdots b_n^{\kappa_n} = \dfrac{d!}{\kappa!} b^\kappa, & x \in \Delta_j\\ 0, & x \notin \Delta_j \end{cases} \tag{14}$$

with $\kappa = (\kappa_0, \kappa_1, \ldots, \kappa_n) \in \mathbb{N}^{n+1}$ a multi-index with properties $\kappa! = \kappa_0!\kappa_1!\cdots\kappa_n!$ and $|\kappa| = \kappa_0 + \kappa_1 + \cdots +$

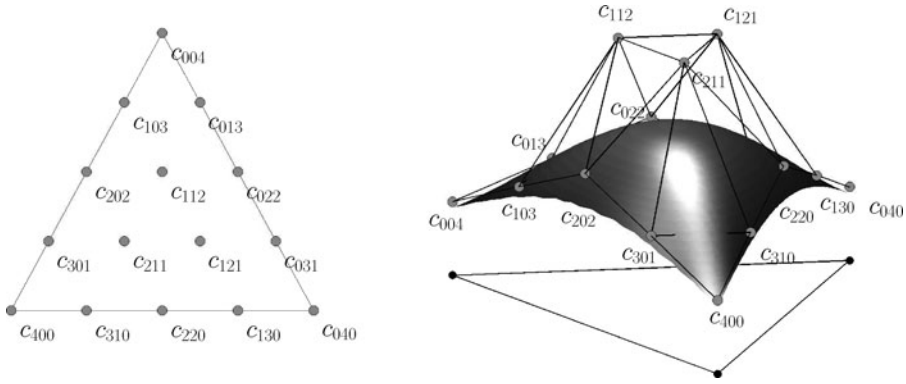

Figure 1. Spatial location B-coefficients for a two-dimensional simplex polynomial of degree 4 (left) and the B-net of the polynomial (right).

κ_n. In de Boor (1987), it is shown that the set

$$\mathcal{B}^d = \left\{B^d_\kappa(b), |\kappa| = d\right\} \tag{15}$$

forms a unique stable local basis for $\mathcal{P}_d$ on Δ. Hence, any simplex polynomial p^{Δ_j} of degree d defined on Δ can be uniquely written as a linear combination of basis polynomials in $\mathcal{B}^d$ (de Boor, 1987)

$$p^{\Delta_j}(x) = \sum_{|\kappa|=d} c_\kappa^{\Delta_j} B^d_\kappa(b) \tag{16}$$

with c_κ the B-coefficients. The total number of valid permutations of κ is $\hat{d} = (d+n)!/n!d!$ which is equal to the total number of B-coefficients per simplex. The B-coefficients have a special property in the sense that they have a unique geometric location inside their parent simplex which are referred to as the domain points. The complete set of domain points ξ_κ in barycentric coordinates of a polynomial of degree d is given by

$$\mathcal{D}_d = \left\{\xi_\kappa = \frac{\kappa}{d},\ |\kappa| = d\right\} \tag{17}$$

which is equal to the location of the unique maximum of the Bernstein basis polynomial B^d_κ in (14). In Figure 1, the domain points and the B-net are shown for a bivariate simplex polynomial of degree 4. The following theorem will be used for the spline approximation of functions over simplices.

Theorem 3.1: *There is a unique polynomial p in n variables of degree d that interpolates any given function f on a n-simplex over the domain points in* (17).

See Chung and Yao (1977) for a proof. The B-form polynomial (16) can also be written in vector form (de Visser, Chu, & Mulder, 2009)

$$p^{\Delta_j}(x) = B^d_{\Delta_j}(x) c^{\Delta_j} \tag{18}$$

with $B^d_{\Delta_j}(x) = [B^d_\kappa(b_{\Delta_j}(x))]_{|\kappa|=d} \in \mathbb{R}^{1\times\hat{d}}$ the vector of basis polynomials and with $c^{\Delta_j} := [c_\kappa^{\Delta_j}]_{|\kappa|=d} \in \mathbb{R}^{\hat{d}\times 1}$ the vector of B-coefficients. Similarly, the globally defined spline function can be written as

$$s(x) = \sum_{j=1}^{J} \sum_{|\kappa|=d} c_\kappa^{\Delta_j} B^d_\kappa(x) = B^d(x) c \tag{19}$$

with $B^d(x) \in \mathbb{R}^{1\times J\hat{d}}$ the global vector of vector basis polynomials and $c \in \mathbb{R}^{J\hat{d}\times 1}$ the global vector of B-coefficients and J the total number of simplices. A spline function is by definition a piecewise-defined polynomial with C^r continuity over the element simplex boundaries. Continuity of order C^r between two neighbouring B-form simplex polynomials p^{Δ_i}, p^{Δ_j} is achieved when all mth-order directional derivatives with $0 \le m \le r$ are equal at every point on the edge $\tilde{\Delta}_{i,j} = \Delta_i \cap \Delta_j$ between the two simplices Δ_i, Δ_j. This is enforced by homogeneous equality constraints of the form $H^{\Delta_i,\Delta_j}[c^T_{\Delta_i}, c^T_{\Delta_j}]^T = 0$ which are defined for every edge of two neighbouring simplices in triangulation $\mathcal{T}$ (Awanou et al., 2005; Lai & Schumaker, 2007, pp. 133–135). This guarantees the existence of a matrix $H \in \mathbb{R}^{R^*\times J\hat{d}}$ with $R^* = rank(H)$ such that $s \in C^r(\Omega)$ if and only if

$$Hc = 0 \tag{20}$$

Constructing H is not trivial and we refer to de Visser et al. (2009) for a general formulation of the continuity conditions and the procedure to derive them utilising a B-net orientation rule.

We next discuss the process of computing integrals and inner products of B-form polynomials which are required for the Galerkin projection. The integral of a B-form basis polynomial of degree d and dimension n for any multi-index $|\kappa| = d$ over the volume of its simplex Δ is given

by

$$\int_\Delta B_\kappa^d(x)dx = \frac{S_\Delta}{\binom{d+n}{n}} \tag{21}$$

where S_Δ is the length (1d), area (2d), volume (3d) or hypervolume of the simplex. Equation (21) leads directly to inner products of any two B-form basis polynomials $B_\gamma^{d_1}, B_\kappa^{d_2}$. Using (14), we have

$$B_\gamma^{d_1} B_\kappa^{d_2} = \frac{d_1!d_2!}{\gamma!\kappa!} b^{\kappa+\gamma}, \quad B_{\gamma+\kappa}^{d_1+d_2} = \frac{(d_1+d_2)!}{(\gamma+\kappa)!} b^{\kappa+\gamma} \tag{22}$$

It follows that

$$\int_\Delta B_\gamma^{d_1} B_\kappa^{d_2} dx = \int_\Delta \frac{d_1!d_2!}{\gamma!\kappa!} \frac{(\gamma+\kappa)!}{(d_1+d_2)!} B_{\gamma+\kappa}^{d_1+d_2} dx \tag{23}$$

which with (21) results in

$$\int_\Delta B_\gamma^{d_1} B_\kappa^{d_2} dx = \frac{d_1!d_2!}{(d_1+d_2)!} \frac{S_\Delta}{\binom{d_1+d_2+n}{n}} \frac{(\gamma+\kappa)!}{\gamma!\kappa!} \tag{24}$$

In the same way, it can be shown that the integral of the product of three B-form basis polynomials $B_\mu^{d_1}$, $B_\gamma^{d_2}$ and $B_\kappa^{d_3}$ is given by

$$\int_\Delta B_\mu^{d_1} B_\gamma^{d_2} B_\kappa^{d_3} dx = \frac{d_1!d_2!d_3!}{(d_1+d_2+d_3)!} \frac{S_\Delta}{\binom{d_1+d_2+d_3+n}{n}} \times \frac{(\mu+\gamma+\kappa)!}{\mu!\gamma!\kappa!} \tag{25}$$

4. Boundary conditions as side constraints

The boundary conditions (1b) are included as side constraints for the B-coefficients which are derived in this section. With standard finite element methods, boundary conditions are commonly explicitly incorporated (Dirichlet type) in the finite-element basis or implicitly incorporated (Neumann type) using a suitable choice for the weak formulation of the PDE. We treat them as side constraints to simplify the construction of the spline basis that satisfies the boundary conditions. No modifications to the spline basis or to the weak formulation are required for different types of boundary conditions. This also allows us to define a model reduction scheme for the general class of linear parabolic PDEs in the next section. The side constraints constrain the spline polynomials at the boundary such that the spline solution satisfies the boundary conditions. The derivation of the constraints requires a new matrix formulation for B-spline derivatives whose image is in the same polynomial space. This allows the formulation of all differential operators in (2) in terms of a single-degree polynomial basis which will also prove to be essential in the model reduction framework. These derivatives are completely defined in terms of a mapping acting on its B-coefficients and are derived by combining the *de Castelau* formulation for the derivatives (de Visser, Chu, & Mulder, 2011) with a polynomial degree raising algorithm (Hu et al., 2007).

We start by introducing a mapping that raises the degree of a simplex polynomial $p \in \mathcal{P}_d$ to $p \in \mathcal{P}_{d+m}$. Let p be a polynomial of degree d defined on a simplex Δ written in the vector form (18), and let c be its coefficients. Then, it can also be evaluated by Hu et al. (2007)

$$B^d(x)c = \frac{d!}{(d+m)!} B^{d+m}(x) A_\Delta^{d+m,d} c \tag{26}$$

with $A_\Delta^{d+m,d} \in \mathbb{R}^{\frac{(d+m+n)!}{n!(d+m)!} \times \frac{(d+n)!}{n!d!}}$ the degree-raising matrix that raises the set of B-coefficients of degree d into a set of B-coefficients of degree $d+m$ (Hu et al., 2007). The right-hand side of (26) is again a B-form polynomial with $B^{d+m}(x)$ the polynomial basis and $\frac{d!}{(d+m)!} A_\Delta^{d+m,d} c$ its B-coefficient vector. It follows that the mapping given by $c \mapsto \frac{d!}{(d+m)!} A_\Delta^{d+m,d} c$ transforms the B-coefficient vector of $p \in \mathcal{P}_d$ to the B-coefficient vector of $p \in \mathcal{P}_{d+m}$.

We next discuss derivatives of B-form polynomials. Let $a = b_{\Delta_j}(v) - b_{\Delta_j}(0) = (a_0, a_1, \ldots, a_n)$ be the directional coordinate of the unit vector v in barycentric coordinates. Then, the general kth-order derivative of a polynomial p of degree $1 \le k \le d$ in the unit directions $v_1, \ldots, v_k$ is given by Lai and Schumaker (2007, p. 29)

$$D_{v_k} \cdots D_{v_1} p(x) = \frac{d!}{(d-k)!} \sum_{|\kappa|=d-k} c_\kappa^{(k)}(a^{(1)}, \ldots, a^{(k)}) B_\kappa^{d-k}(x) \tag{27}$$

where $c_\kappa^{(k)}(a^{(1)}, \ldots, a^{(k)})$ are the quantities obtained after carrying out k steps of the de Castelau iteration

$$c_\kappa^{(k)}(a) = \sum_{|\gamma|=1} a^\gamma c_{\kappa+\gamma}^{(k-1)}(a), \quad |\kappa| = d-k, k \le d \tag{28}$$

using the directional coordinates $a^{(1)}, \ldots, a^{(k)}$ of $v_1, \ldots, v_k$ in that order. For example, if we put $d_\kappa = c_\kappa^{(1)}(a^{(1)})$, then $c_\kappa^{(2)}(a^{(1)}, a^{(2)}) = d_\kappa^{(1)}(a^{(2)})$. Equation (28) can be written in matrix form (de Visser et al., 2011)

$$c^{(k)} = P^{d-k,d-k+1}(a) c^{(k-1)}(a) \tag{29}$$

with $P^{d-k,d-k+1} \in \mathbb{R}^{\frac{(d-k+n)!}{n!(d-k)!} \times \frac{(d-k+1+n)!}{n!(d-k+1)!}}$ the one-step de Castelau matrix (de Visser et al., 2011) which reduces the set of B-coefficients of degree $d-k+1$ into a set of B-coefficients of degree $d-k$. Using the vector formulation of the B-form polynomial (18) and the de Castelau

algorithm (29), the general derivative (27) can be written in matrix form

$$D^k p(x) = \frac{d!}{(d-k)!} B^{d-k}(x) P^{d-k,d}(a^{(1)}, \ldots, a^{(k)}) c \tag{30}$$

with $D^k = D_{v_k} \ldots D_{v_1}$ and

$$P^{d-k,d}(a^{(1)}, \ldots, a^{(k)}) = \Pi_{i=1}^{k} P^{d-i,d-i+1}(a^{(i)}) \tag{31}$$

a multi-degree de Castelau matrix. Equation (30) can be combined with polynomial degree raising (26) to construct kth-order derivatives whose image is in $\mathcal{P}_{d-k+m}$.

Theorem 4.1: *Let $p \in \mathcal{P}_d$ be a B-form polynomial of degree $1 \leq k \leq d$ relative to simplex Δ, and given a set of directions $v_1, \ldots, v_k$ described by the directional coordinates $a^{(k)} = (a_0^{(k)}, \ldots, a_n^{(k)})$. The matrix form of the kth-order derivative $D^k = D_{v_k} \cdots D_{v_1} p \in \mathcal{P}_{d-k+m}$ in the unit directions $v_1, \ldots, v_k$ is given by*

$$D^k p(x) = \frac{d!}{(d-k+m)!} B^{d-k+m}(x) \times A_{\Delta}^{d-k+m,d-k} P^{d-k,d}(a^{(1)}, \ldots, a^{(k)}) c \tag{32}$$

Proof: The right-hand side of (30) is a B-form polynomial in $\mathcal{P}_{d-k}$ with $B^{d-k}(x)$ its polynomial basis and $c^{(k)} = \frac{d!}{(d-k)!} P^{d-k,d}(a^{(1)}, \ldots, a^{(k)}) c$ its coefficients. Applying the mapping $c^{(k)} \mapsto \frac{(d-k)!}{(d-k+m)!} A^{d-k+m,d-k} c^{(k)}$ to (30) to raise $D^k p(x) \in \mathcal{P}_{d-k}$ to $D^k p(x) \in \mathcal{P}_{d-k+m}$ gives the result in (32). ■

The spline function $s \in S_d^r(\Omega)$ is guaranteed to be r-times continuously differentiable on the domain Ω. The following corollary introduces a mapping for the B-coefficient vector to compute derivatives of s and follows directly from Theorem 4.1.

Corollary 4.1: *Given the B-coefficient vector c of $s \in S_d^r(\mathcal{T})$, the mapping $c \mapsto \mathbb{T}_{D^k}^{d-k+m,d} c$ with*

$$\mathbb{T}_{D^k}^{d-k+m,d} = diag\left(\frac{d!}{(d-k+m)!} \times A_{\Delta}^{d-k+m,d-k} P^{d-k,d}(a^{(1)}, \ldots, a^{(k)}) \right)_{j=1}^{J} \tag{33}$$

maps the B-coefficients of $s \in S_d^r(\mathcal{T})$ to the B-coefficients of $D^k s \in S_{d-k+m}^{r-k}(\mathcal{T})$, that is

$$D^k[B^d(x)c] = B^{d-k+m}(x) \mathbb{T}_{D^k}^{d-k+m,d} c \tag{34}$$

Hence, any spatial derivative can simply be constructed by applying the mapping (33) in parameter space. Note that the spatial derivative D^α (3) of order $|\alpha|$ is a special case of D^k. Corollary 4.1 is used to define a similar transformation matrix for the general linear differential operator (2) with constant coefficients.

Theorem 4.2: *Let L be a linear partial differential operator of order k given by (2) with constant coefficients and given the B-coefficient vector c of $s \in S_d^r(\mathcal{T})$. Furthermore, let $\mathbb{T}_{D^\alpha}^{d,d}$ be the transformation matrix that maps $s \in S_d^r(\mathcal{T})$ to $D^\alpha s \in S_d^{r-|\alpha|}(\mathcal{T})$ constructed using (33) with $k = m = |\alpha|$. Then, the mapping $c \mapsto \mathbb{T}_L^{d,d} c$ with*

$$\mathbb{T}_L^{d,d} = \sum_{|\alpha| \leq k} a_\alpha \mathbb{T}_{D^\alpha}^{d,d} \tag{35}$$

maps the B-coefficients of $s \in S_d^r(\mathcal{T})$ to the B-coefficients of $Ls \in S_d^{r-k}(\mathcal{T})$, that is, $L[B^d(x)c] = B^d(x) \mathbb{T}_L^{d,d} c$.

Proof: Applying Corollary 4.1, the linear operator acting on s can be written in terms of a single degree basis polynomial

$$\begin{aligned} L\left[B^d(x)c\right] &= \sum_{|\alpha| \leq k} a_\alpha D^\alpha \left[B^d(x)c\right] \\ &= \sum_{|\alpha| \leq k} a_\alpha B^d(x) \mathbb{T}_{D^\alpha}^{d,d} c \end{aligned} \tag{36}$$

which can be written in the form $L\left[B^d(x)c\right] = B^d(x) \mathbb{T}_L^{d,d} c$, where $\mathbb{T}_L^{d,d}$ is given by (35). ■

This theorem is used to define the boundary constraints. The value of a B-form simplex polynomial at the edge of the simplex is uniquely determined by the values of the B-coefficients located on the edge (Awanou & Lai, 2004) (see also Figure 1). This implies that there is a matrix D which maps the B-coefficients of s to the B-coefficients of $s|_\Gamma$, that is, $s|_\Gamma = \tilde{B}^d(x) D c$, with $\tilde{B}^d(x)$ an $n-1$ B-form vector basis (Awanou & Lai, 2004). Or, in other words, the action $c \mapsto Dc$ selects the B-coefficients located on the boundary. Combined with Theorem 4.2, it follows that $c \mapsto D \mathbb{T}_{L_\Gamma}^{d,d} c$ maps the B-coefficients of s to the B-coefficients of $L_\Gamma s|_\Gamma$, that is, $L_\Gamma s|_\Gamma = \tilde{B}^d(x) D \mathbb{T}_{L_\Gamma}^{d,d} c$. Furthermore, by Theorem 3.1, there is a unique $n-1$-dimensional simplex polynomial that interpolates the actuator distribution functions $g_{\Gamma,i}(x)$ at the domain points on the simplex face located on the boundary Γ. Denote g_Γ^i as the B-coefficient vector of the $n-1$-dimensional spline function that interpolates $g_{\Gamma,i}(x)$ over the complete set of domain points on the boundary Γ and define $G_\Gamma = \left[g_\Gamma^1 \cdots g_\Gamma^m\right]$, and therefore we may set

$$D \mathbb{T}_{L_\Gamma}^{d,d} c(t) = G_\Gamma u_\Gamma(t) \tag{37}$$

to enforce that the spline solution satisfies the boundary condition (1b) approximately. Note that in the case of homogeneous boundary conditions, the B-coefficient

constraints model the boundary conditions exactly since no approximations are involved.

5. Model reduction of linear parabolic PDEs

In this section, the finite-dimensional state-space description of (1) is constructed using multivariate splines. First, the DPS is reduced to a finite set of coupled ODEs using Galerkin projection after which the complete system of equations including the side constraints for the smoothness conditions (20) and boundary conditions (37) is transformed to state-space format using a null space approach that significantly reduces the size of the system.

The spline approximation is determined through the following Galerkin-type weak formulation: Find $y(x,t) \in \mathcal{L}^2\left(0, T; \mathcal{H}^k(\Omega)\right)$ such that

$$\int_\Omega \frac{\partial y(x,t)}{\partial t} v(x)dx = \int_\Omega (Ly(x,t) + g(x)u(t))v(x)dx$$
$$L_\Gamma y(x,t) = g_\Gamma(x)u_\Gamma(t), \quad \text{on } \Gamma_T \tag{38}$$

$\forall v \in \mathcal{V}_0$ and $t \in [0, T]$, with $\mathcal{H}^k(\Omega)$ the standard Sobolev space consisting of all functions whose spatial derivatives up to k-th order exist in the weak sense and are in $\mathcal{L}^2(\Omega)$ and with $\mathcal{V}_0$ the space associated with the test functions $v(x)$

$$\mathcal{V}_0 = \left\{v \in \mathcal{H}^k(\Omega) : L_\Gamma v = 0\right\} \tag{39}$$

A common approach is to apply integration by parts and the Gauss–Green theorem to (38) to lower the smoothness requirements and to implicitly incorporate natural (Neumann type) boundary conditions in the weak formulation. This approach is not employed here since a spline basis of higher degree and smoothness with the characteristics of the strong solution can easily be constructed.

We now define the spline approximation of (38). Let $\mathcal{T}$ be the triangulation of Ω if Ω is a polygonal domain. Otherwise, we choose the vertices on Γ such that $\mathcal{T}$ becomes the approximation of Ω. Let d and r be two positive integers with $d > r$, $r \geq k-1$ and let $\mathcal{S}$ be a spline subspace consisting of spline functions which are C^r inside Ω. We have that $\mathcal{S} \subset S_d^{k-1}(\mathcal{T}) \subset \mathcal{H}^k(\Omega)$. The finite-dimensional approximation of y in Ω can be represented by

$$y^N(x,t) = s(x,t) = \sum_{j=1}^{J} \sum_{|\kappa|=d} c_\kappa^{\Delta_j}(t) B_\kappa^d(x) = B^d(x)c(t) \tag{40}$$

with $s \in \mathcal{S}$, $N = J\hat{d}$ and where the B-coefficients satisfy the C^r continuity conditions (20). In (40), the B-form basis polynomials $B_\kappa^d(x)$ are used as spatial basis functions and the B-coefficients as time-varying expansion coefficients. Let $\mathcal{S}_0 = \mathcal{S} \cap \mathcal{V}_0$. The spline approximation of (38) with respect to the spatial variables is $s(\cdot, t) \in \mathcal{S}$ which must satisfy the approximate boundary conditions (37) such that

$$\int_\Omega \frac{\partial s(x,t)}{\partial t} s_v(x)dx = \int_\Omega (Ls(x,t) + g(x)u(t))s_v(x)dx \tag{41}$$

$\forall s_v \in \mathcal{S}_0$ and $t \in [0\ \ T]$. Recall from Theorem 4.2 that the differential operator acting on s can be written in terms of a single-degree basis polynomial

$$L\left[B^d(x)c(t)\right] = \sum_{|\alpha|\leq k} a_\alpha(x) B^d(x) \mathbb{T}_{D^\alpha}^{d,d} c(t) \tag{42}$$

with $\mathbb{T}_{D^\alpha}^{d,d}$ the transformation matrix that maps the B-coefficient vector of $s \in S_d^r(\mathcal{T})$ to the B-coefficients of $D^\alpha s \in S_d^{r-|\alpha|}(\mathcal{T})$. Let c_v be the B-coefficient vector of the test function $s_v \in \mathcal{S}_0$ with $s_v = B^d(x)c_v$, (41) can be written as

$$c_v^T \left(\int_\Omega \left[B^d(x)\right]^T B^d(x)dx\right) \dot{c}(t)$$
$$= c_v^T \left[\sum_{|\alpha|\leq k} \left(\int_\Omega a_\alpha(x) \left[B^d(x)\right]^T B^d(x)dx\right) \mathbb{T}_{D^\alpha}^{d,d}\right] c(t)$$
$$+ c_v^T \left(\int_\Omega \left[B^d(x)\right]^T g(x)dx\right) u(t) \tag{43}$$

which must hold for all B-coefficient vectors c_v of splines in $\mathcal{S}_0$, that is, for all c_v satisfying the C^r smoothness constraints $Hc_v = 0$ and the homogeneous boundary constraints $D\mathbb{T}_{L_\Gamma}^{d,d} c_v = 0$. Equation (43) is written in terms of B-form polynomials by approximating the actuator distribution functions $g_i(x)$ and the PDE coefficients $a_\alpha(x)$ using B-splines. If these functions are continuous, interpolation is the obvious choice. By Theorem 3.1, there is a unique simplex polynomial that interpolates $a_\alpha(x)$ over the simplex domain points $\{\xi_\kappa^\Delta, |\kappa| = d\}$. Let a^α be a B-coefficient vector with $s_{a_\alpha}(x) = B^d(x)a^\alpha \in S_d^0(\mathcal{T})$ the spline interpolation of $a_\alpha(x)$ over the complete set of domain points and let g^i be a B-coefficient vector with $s_{g_i}(x) = B^d(x)g^i \in S_d^0(\mathcal{T})$ the spline interpolation of $g_i(x)$ and define $G = [g^1, g^2, \cdots, g^m]$, then, the projection condition (43) can be approximated in terms

of B-form polynomials by

$$c_v^T\left(\int_\Omega [B^d(x)]^T B^d(x)dx\right)\dot{c}(t) = c_v^T\left[\sum_{|\alpha|\le k}\left(\int_\Omega B^d(x)a^\alpha\left[B^d(x)\right]^T B^d(x)dx\right)\mathbb{T}_{D^\alpha}^{d,d}\right]c(t) + c_v^T\left(\int_\Omega [B^d(x)]^T B^d(x)dx\right)Gu(t) \quad (44)$$

If $a_\alpha(x)$ and $g_i(x)$ are not continuous, interpolation can still be used except that the interpolation values should come from a suitable continuous approximation of $a_\alpha(x)$ and $g_i(x)$ or one can use a piecewise discontinuous polynomial approximation using, for example, a least squares fit (de Visser et al., 2009).

The integral over a simplex Δ of the product of two or more basis polynomials defined on different simplices is always equal to zero because of their local support. It follows that the integrals in (44) result in block-diagonal matrices. Applying the integration gives

$$c_v^T M\dot{c}(t) = c_v^T\left(\sum_{|\alpha|\le k} K^\alpha \mathbb{T}_{D^\alpha}^{d,d}\right)c(t) + c_v^T MGu(t) \quad (45)$$

with $M = diag(M_\Delta)$ a mass matrix (Awanou & Lai, 2004) with blocks

$$M_\Delta = \left[\int_\Delta B_\kappa^d(x)B_\gamma^d(x)dx\right]_{\substack{|\kappa|=d\\|\gamma|=d}} \quad (46)$$

and $K^\alpha = diag(K_\Delta^\alpha)$ a bending matrix with blocks

$$K_\Delta^\alpha = \left[\int_\Delta B^d(x)a^\alpha B_\kappa^d(x)B_\gamma^d(x)dx\right]_{\substack{|\kappa|=d\\|\gamma|=d}} = \left[\int_\Delta \sum_{|\mu|=d} B_\mu^d(x)a_\mu^\alpha B_\kappa^d(x)B_\gamma^d(x)dx\right]_{\substack{|\kappa|=d\\|\gamma|=d}} \quad (47)$$

Using (24) and (25), the mass and bending matrices can be explicitly calculated with

$$M_\Delta = \frac{d!d!}{(2d)!}\frac{S_\Delta}{\binom{2d+n}{n}}\left[\frac{(\gamma+\kappa)!}{\gamma!\kappa!}\right]_{\substack{|\kappa|=d\\|\gamma|=d}} \quad (48)$$

$$K_\Delta^\alpha = \frac{d!d!d!}{(3d)!}\frac{S_\Delta}{\binom{3d+n}{n}}\left[\sum_{|\mu|=d} a_\mu^\alpha\frac{(\mu+\gamma+\kappa)!}{\mu!\gamma!\kappa!}\right]_{\substack{|\kappa|=d\\|\gamma|=d}} \quad (49)$$

Let $K = \sum_{|\alpha|\le k} K^\alpha \mathbb{T}_{D^\alpha}^{d,d}$ and $F = MG$, it follows that the B-coefficient vector c of the spline approximation satisfies

$$c_v^T M\dot{c}(t) = c_v^T Kc(t) + c_v^T Fu(t) \quad (50a)$$

$$Hc(t) = 0 \quad (50b)$$

$$D\mathbb{T}_{L_\Gamma}^{d,d}c(t) = G_\Gamma u_\Gamma(t) \quad (50c)$$

for all B-coefficient vectors c_v of splines in $\mathcal{S}_0$ satisfying $Hc_v = 0$ and $D\mathbb{T}_{L_\Gamma}^{d,d}c_v = 0$. Existence and uniqueness of c can be shown by using the same argument for the existence of the weak solution satisfying (38) (Awanou et al., 2005; Lai & Wenston, 2004). We are interested in solving (50) for $\dot{c}$. A null-space approach is proposed which significantly reduces the size of the system by the rank of the side constraints. Let $Q=[H^T\ (D\mathbb{T}_{L_\Gamma}^{d,d})^T]^T$ and $\bar{G}_\Gamma = [0^T\ G_\Gamma^T]^T$, the constraints (50b) and (50c) can be written as

$$Qc(t) = \bar{G}_\Gamma u_\Gamma(t) \quad (51)$$

Let V be a basis for $null(Q)$ such that $QV = 0$ and let $c_p(t) = C_p u_\Gamma(t)$ be a particular solution of (51). The general solution set for (51) can be written as

$$c(t) = V\tilde{c}(t) + C_p u_\Gamma(t) \quad (52)$$

with $\tilde{c} \in \mathbb{R}^{N-R^*}$ the coordinate vector of c relative to the basis for $null(Q)$ and with R^* the rank of Q. Since $Qc_v = 0$ for all B-coefficient vectors c_v of splines in $\mathcal{S}_0$, the solution set for c_v can be written as $c_v = V\tilde{c}_v$. Substituting this set for c_v and the solution set (52) for c in (50) gives

$$\tilde{c}_v^T V^T M(V\dot{\tilde{c}}(t) + C_p\dot{u}_\Gamma(t)) = \tilde{c}_v^T V^T K(V\tilde{c}(t) + C_p u_\Gamma(t)) + \tilde{c}_v^T V^T Fu(t) \quad (53)$$

which is a reduced unconstrained system of order $N - R^*$ projected on the null space of the side constraints. Since (53) must hold for all $\tilde{c}_v$, (53) is equivalent to

$$\left(V^T MV\right)\dot{\tilde{c}}(t) = V^T\left[KV\tilde{c}(t) + KC_p u_\Gamma(t) + Fu(t) - MC_p\dot{u}_\Gamma(t)\right] \quad (54)$$

The null-space method requires the construction of the null basis V for Q. We use the sparse null-space algorithm recently introduced in Hölzel and Bernstein (2014) which is particularly useful for computing the null space of large sparse matrices. The particular solution is obtained as by-product of the computations necessary to obtain V. For the measured output (1c) and the controlled output (1d), the null-space Galerkin method yields

$$z_{m_k}(t) = B^d(x_k)\mathbb{T}_{L_{z_m}}^{d,d}\left[V\tilde{c}(t) + C_p u_\Gamma(t)\right] \quad (55)$$

$$z_{c_i}(t) = (\phi^i)^T M\mathbb{T}_{L_{z_c}}^{d,d}[V\tilde{c}(t) + C_p u_\Gamma(t)] \quad (56)$$

where $\mathbb{T}^{d,d}_{L_z}$ maps the B-coefficient vector of s to the B-coefficient vector of $L_z s$ and with ϕ^i the B-coefficient vector of the spline that interpolates $\phi_i(x)$. Finally, we obtain the system in state-space format

$$\begin{aligned} \dot{x}^N(t) &= Ax^N(t) + B\bar{u}(t) \\ z^N_{m_k}(t) &= C_{m_k}x^N(t), \quad z^N_{c_i}(t) = C_{c_i}x^N(t) \end{aligned} \tag{57}$$

where

$$\begin{aligned} x^N(t) &= \left[\tilde{c}^T(t)\ u^T_\Gamma(t)\right]^T, \quad \bar{u}(t) = \left[u^T(t)\ \dot{u}^T_\Gamma(t)\right]^T \\ A &= \begin{bmatrix} \left(V^TMV\right)^{-1}V^TKV & \left(V^TMV\right)^{-1}V^TKC_p \\ 0 & 0 \end{bmatrix} \\ B &= \begin{bmatrix} \left(V^TMV\right)^{-1}V^TF & -\left(V^TMV\right)^{-1}V^TMC_p \\ 0 & I \end{bmatrix} \\ C_{m_k} &= \begin{bmatrix} B^d(x_k)\mathbb{T}^{d,d}_{L_{z_m}}V & B^d(x_k)\mathbb{T}^{d,d}_{L_{z_m}}C_p \end{bmatrix} \\ C_{c_i} &= \begin{bmatrix} (\phi^i)^TM\mathbb{T}^{d,d}_{L_{z_c}}V & (\phi^i)^TM\mathbb{T}^{d,d}_{L_{z_c}}C_p \end{bmatrix} \end{aligned} \tag{58}$$

Remark 5.1: The approximation power of the general multivariate spline space $S^r_d(\mathcal{T})$ is not fully known. For bi-variate spline spaces, full approximation power in all p-norms is achieved when $d \geq 3r+2$ (Lai & Schumaker, 1998; Lai & Schumaker, 2007, pp. 276–286). The orthogonality of the Galerkin projection (41) ensures that the approximation y^N is the best possible solution in the space spanned by the basis functions. Specific bounds for the $\mathcal{L}_2$ norm of projections onto bi-variate spline spaces $S^0_d(\mathcal{T})$ and $S^d_d(\mathcal{T})$ with $d \geq 3r+2$ are derived in Von Golitschek and Schumaker (2002).

6. Controller synthesis

The reduced-order model (57) can be used to design any suitable linear controller. In this study, a quadratic optimal design is considered where the controlled output (56) is used to build the objective function (11). The quadratic objective function (11) for the reduced-order model becomes

$$\mathcal{J} = \int_0^\infty \left(x^N\right)^T C_c^TC_cx^N + \bar{u}^TR\bar{u}\,dt \tag{59}$$

Assuming that (A, B) is stabilisable, the state feedback $\bar{u}(t) = -K_cx^N(t)$ that minimises (59) can be computed by solving the associated algebraic Ricatti equation for (59). An output feedback controller is obtained by combining the state feedback with a state observer and takes the form

$$\begin{aligned} \bar{u}(t) &= -K_c\hat{x}^N(t) \\ \dot{\hat{x}}^N(t) &= A\hat{x}^N + B\bar{u}(t) + K_o(z_m(t) - \hat{z}^N_m(t)) \\ \hat{z}^N_m(t) &= C_m\hat{x}^N(t), \qquad \hat{x}^N(0) = \hat{x}^N_0 \end{aligned} \tag{60}$$

where the observer gain K_o is tuned such that $A - K_oC_m$ has desired stability margins. The closed-loop system consists of the actual DPS (9) combined with the controller (60)

$$\begin{bmatrix} \dot{x} \\ \dot{\hat{x}}^N \end{bmatrix} = \begin{bmatrix} \bar{\mathcal{A}} & -\bar{\mathcal{B}}K_c \\ K_o\bar{\mathcal{C}}_m & A - BK_c - K_oC_m \end{bmatrix} \begin{bmatrix} x \\ \hat{x}^N \end{bmatrix} \tag{61}$$

When using reduced-order models in the design of a control system, the truncated dynamics must be taken into account in the stability analysis. Robustness with respect to the truncated dynamics of reduced-order controllers based on projections on non-modal subspaces, such as finite-element spaces and spline spaces, for the linear class of parabolic DPS treated in this paper has been discussed in Balas (1983). In Balas (1983), precise conditions are derived under which model reduction based on consistent Galerkin approximations will lead to stable infinite-dimensional control. In particular, provided that the infinite-dimensional system is exponentially stable and N sufficiently large, a controller which exponentially stabilises the closed-loop ODE system also stabilises the closed-loop parabolic PDE system. The assumption that the DPS is exponentially stable is generally required in order to prove that the estimates are bounded for all times, that is $\|y - y^N\|_2 \leq \mu(N)$, $\forall t$ with $\mu(N)$ a positive number depending on N satisfying $\lim_{N\to\infty}\mu(N) = 0$ (Balas, 1983; Baker et al., 2000). In the next section, we apply the reduction method to control two unstable PDEs and analyse the closed-loop stability by computing the eigenvalues of (61) numerically. To compute the eigenvalues and to simulate the response of the system, an accurate high-order model is used to represent the actual DPS, that is, $\bar{\mathcal{A}}$, $\bar{\mathcal{B}}$ and $\bar{\mathcal{C}}_m$ in (61), and lower order models are used to design the control system. For a given partitioning of the domain, the degree and order of continuity of the spline basis can be chosen arbitrarily to derive these state space models. The order of continuity is chosen equal to the continuity of the strong solution of the PDE system. For the systems considered in the next section, the strong solution is C^2 smooth. The degree of the control model can subsequently be tuned to obtain a desirable trade-off between the order of the model and the accuracy of the model, and thereby closed-loop performance. We provide a closed-loop performance analysis for various degrees and selected the model that gives a good balance between model order and performance to implement the controller.

7. Demonstration

In this section, two representative PDE control problems are presented to demonstrate the implementation and to evaluate the effectiveness of the proposed model reduction scheme. In the first case, we consider stabilisation of a 1-D unstable reaction diffusion process which is often considered as a benchmark problem (see e.g. Smyshlyaev & Krstic, 2004). For this problem, an analytic solution of the spatial differential operator eigenvalue problem is available which allows for a direct comparison of the eigenvalues and stability eigenfunctions of the reduced-order models with the analytic solution. In the second case, stabilisation of a 2-D reaction–convection–diffusion equation on an irregular spatial domain is considered for which analytic solutions of the spatial differential operator eigenvalue problem are not possible. This is a non-trivial example which better illustrates the potential of the spline reduction framework. We provide numerical convergence results for increasing polynomial degrees and show that effective feedback stabilisation can be achieved using low-order control models.

7.1 Boundary feedback stabilisation of an unstable reaction–diffusion equation

In this demo, boundary feedback control of an unstable reaction–diffusion equation with constant coefficients is considered

$$\begin{cases} \frac{\partial y(x,t)}{\partial t} = \mu \frac{\partial^2 y(x,t)}{\partial x^2} + a y(x,t) & \text{in } (0,1)\times(0,\infty) \\ y(0,t) = 0, \quad y(1,t) = u(t) & \text{in } (0,\infty) \\ y(x,0) = sin(\pi x) & \text{in } (0,1) \\ z_m(t) = \frac{\partial y(0,t)}{\partial x} & \text{in } (0,\infty) \\ z_{c_1}(t) = \int_\Omega sin(\pi x) y(x,t) dx & \text{in } (0,\infty) \\ z_{c_2}(t) = \int_\Omega sin(2\pi x) y(x,t) dx & \text{in } (0,\infty) \end{cases} \tag{62}$$

Table 1. Number of system states ($J\hat{d} - R^* + 1$).

Degree	3	4	5	6	7	8	9	10
$\mathcal{T}_3$	5	8	11	14	17	20	23	26
$\mathcal{T}_6$	8	14	20	26	32	38	44	50

where $\frac{\partial y}{\partial x}(0,t)$ is measured and $y(1,t)$ is actuated. The coefficients are chosen as $\mu = 0.2$, $a = 4$. The complete system is converted to state-space format using a $C^2(\Omega)$ continuous spline basis of various degrees defined on a uniform partitioning of the domain consisting of three and six simplices. The dimension of the state-space systems is listed in Table 1. For system (62), the differential operator is of the form $\mathcal{A}y = \mu \frac{\partial^2 y}{\partial x^2} + ay$ and the exact solution of the differential operator eigenvalue problem $\mathcal{A}\phi_j(x) = \lambda_j \phi_j(x)$ is given by (Curtain and Zwart, 1995)

$$\lambda_j = a - \mu j^2 \pi^2, \quad \phi_j(x) = sin\left(j\pi x\right) \tag{63}$$

with $j = 1, 2, \ldots, \infty$, λ_j the eigenvalues and ϕ_j the eigenfunctions. The case with $\mu = 0.2$, $a = 4$ corresponds to one unstable eigenvalue at $\lambda_1 = 4 - 0.2\pi^2 \approx 2.03$. Using this eigenfunction expansion, we can directly calculate the power spectral density (PSD) of the differential operator (Jovanović & Bamieh, 2006)

$$\|(i\omega - \mathcal{A})^{-1}\|_{HS}^2 = \|\mathcal{F}(\omega)\|_{HS}^2 = \sum_{j\in\mathbb{N}} \frac{1}{\omega^2 + \lambda_j^4} \tag{64}$$

where $\|\cdot\|_{HS}$ denotes the Hilbert–Schmidt norm (generalisation of the Frobenius norm for matrices). Figure 2 shows the errors for the first four dominant eigenvalues of the reduced-order models and Figure 3 compares the PSD. It can be observed that the dominant modes converge quickly up to numerical precision and that the reduced-order models only deviate at higher frequencies.

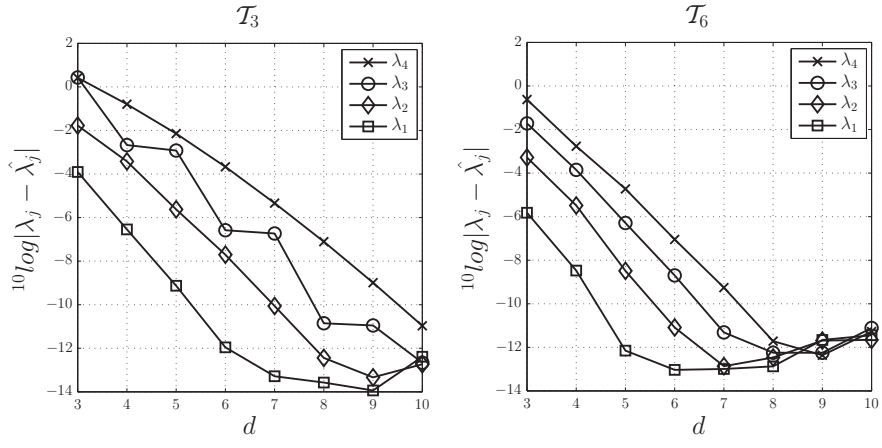

Figure 2. The error of the first four dominant eigenvalues of the $S_d^2(\mathcal{T}_3)$ and $S_d^2(\mathcal{T}_6)$ reduced-order models.

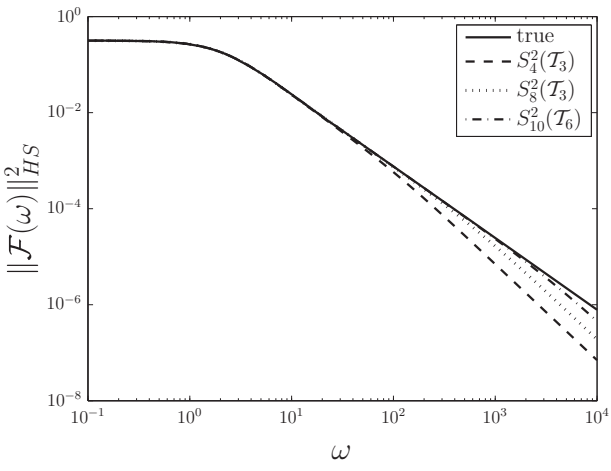

Figure 3. Power spectral density of the differential operator of the reduced-order models compared with the analytic solution.

The control objective is to stabilise the state at its unstable equilibrium $\bar{y} = 0$. The controller (60) is synthesised using $s \in S_d^2(\mathcal{T}_3)$ Galerkin models of various degrees. The controlled output is built using the first two dominant eigenfunctions $\phi_1(x)$, $\phi_2(x)$ and the input weight is set to $R = 0.01$. Adding more eigenfunctions to the controlled output or lowering the input weight did not further improve the performance of the controller. An $s \in S_{10}^2(\mathcal{T}_6)$ Galerkin model is assumed to represent the original DPS, that is, $\bar{\mathcal{A}}$, $\bar{\mathcal{B}}$, $\bar{\mathcal{C}}_m$ in (61), and is used in the simulations. It is verified that further increase of the order provided no improvement on the accuracy of the results. The real part of the two least stable eigenvalues (pairs) of the closed-loop system (61) is shown in Table 2. Higher degree controllers give a faster stabilisation but no significant improvement is achieved after $d = 4$; the dominant dynamics are accurately captured by low-degree models. The closed-loop response for the $s \in S_4^2(\mathcal{T}_3)$ model-based controller is shown in Figure 4. It can be observed that the

Table 2. Real part of the two least stable eigenvalues of the closed-loop system (61).

Degree	3	4	5	6	7	8
σ_1	−1.41	−2.47	−2.62	−2.69	−2.69	−2.69
σ_2	−1.56	−3.29	−3.06	−3.09	−3.10	−3.10

$s \in S_4^2(\mathcal{T}_3)$ model-based controller provides a satisfactory performance and quickly stabilises the system.

7.2 In-domain control of a reaction–convection–diffusion equation

In this demo, in-domain feedback control of a reaction–convection–diffusion equation is considered with spatially varying coefficients

$$\begin{cases} \frac{\partial y(x,t)}{\partial t} = \mu(x)\nabla^2 y(x,t) - \upsilon(x)\cdot\nabla y(x,t) \\ \qquad\qquad +a(x)y(x,t) + g(x)u(t) & \text{in } \Omega_T \\ \frac{\partial y(x,t)}{\partial n} = 0 & \text{on } \Gamma \\ y(x,0) = 5\cos\left(\pi\left(x_1^2-1\right)\left(x_1^2-0.09\right)\right) \\ \qquad\qquad -5\cos\left(\pi\left(x_2^2-1\right)\left(x_2^2-0.09\right)\right) \\ z_{m_k}(t) = z_{c_k}(t) = y(x_k,t), & k = 1,\ldots,4 \end{cases} \tag{65}$$

on a rectangular domain with a cut-out

$$\Omega = \{(x_1,x_2)\,,\,(x_1,x_2) \in (-1,1) \times (-1,1) \setminus (-0.3,0.3)\times(-0.3,0.3)\}$$

A rotating velocity field is applied with $\upsilon(x) = [\,x_2\ -x_1\,]^T$, the diffusivity is kept constant $\mu(x) = \mu = 0.05$ and the reaction rate is chosen as $a(x) = 0.5\cos(\frac{1}{2}\pi x_1)e^{x_2}$ which has a destabilising effect. The system is controlled using four actuators whose spatial distributions are modelled as Gaussian radial basis functions: $g_i(x) = exp[-(\|x - x_c\|_2^2)/(2\sigma^2)]$

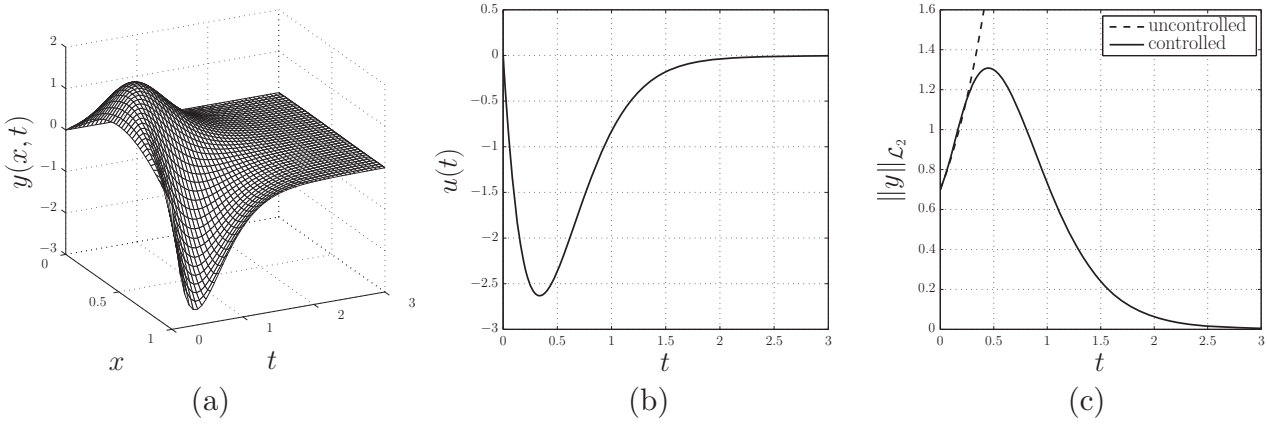

Figure 4. Closed-loop response of the $s \in S_4^2(\mathcal{T}_3)$ controller. An $s \in S_{10}^2(\mathcal{T}_6)$ Galerkin model is used for simulating the response. (a) Response, (b) boundary control input, (c) $\mathcal{L}_2$ norm of the state.

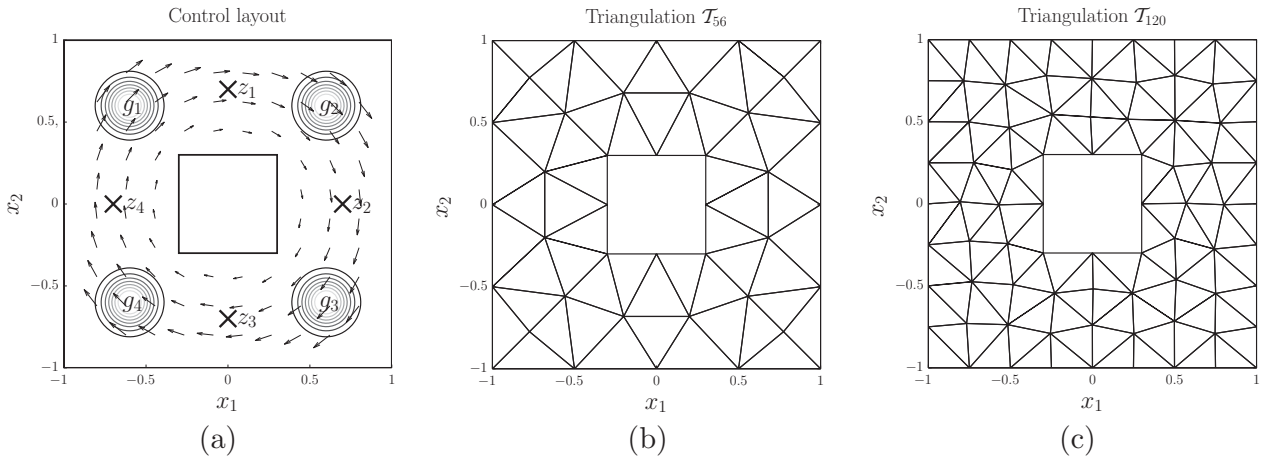

Figure 5. Control layout and triangulations. (a) Domain, convective field $v(x)$, actuator distribution contours $g_i(x)$ and sensor locations z_i. (b) Triangulation with 56 simplices used for control design. (c) Triangulation with 120 simplices used for simulation.

Table 3. Dimension state-space systems.

(a) Number of states $J\hat{d} - R^*$

Degree	4	5	6	7	8	9	10
$\mathcal{T}_{56}$	18	114	266	474	738	1058	1434
$\mathcal{T}_{120}$	32	232	552	992	1552	2232	3032

(b) State reduction R^*

$\mathcal{T}_{56}$	822	1062	1302	1542	1782	2022	2262
$\mathcal{T}_{120}$	1768	2288	2808	3328	3848	4368	4888

and four in-domain Dirichlet measurements are used for feedback. The complete geometry is shown in Figure 5 along with the triangulations used in this study. All state-space models are derived using a C^2 continuous spline basis of various degrees defined on a triangulation consisting of 56 and 120 simplices. The dimension of the state-space systems are listed in Table 3(a) and the size reduction R^* resulting from the null-space projection is listed in Table 3(b).

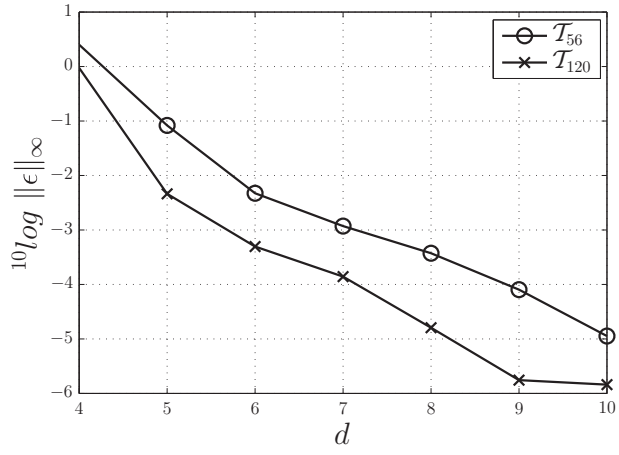

Figure 6. The maximum error versus degrees on $\mathcal{T}_{56}$ and $\mathcal{T}_{120}$ with respect to the manufactured solution.

Since no analytic solution is available, the state-space systems are validated using a manufactured solution (Roache, 2002). For this, we consider the system (65) with

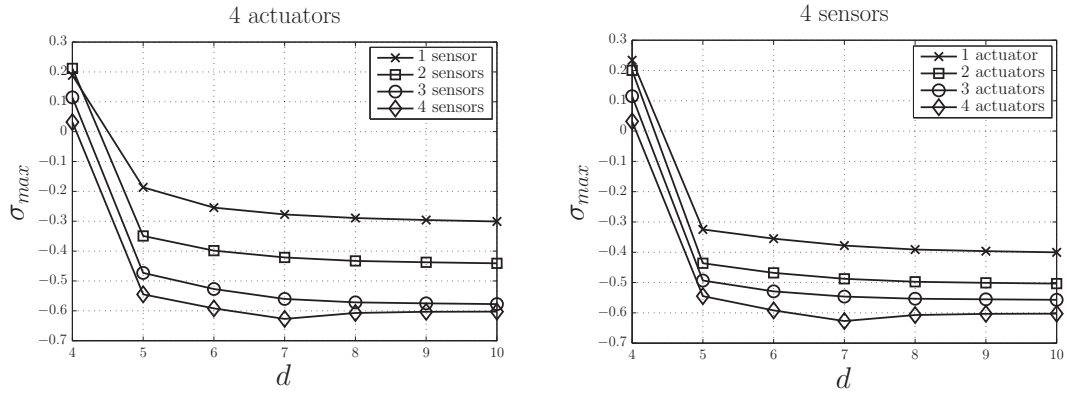

Figure 7. Real part of the least stable eigenvalue of the closed-loop system (61) with $R = diag(0.01)$. An $s \in S_9^2(\mathcal{T}_{120})$ model is used as the 'true system'. Left: $s \in S_d^2(\mathcal{T}_{56})$ controllers using four actuators with one (z_1), two (z_1, z_3), three (z_1, z_2, z_3) and four sensors. Right: $s \in S_d^2(\mathcal{T}_{56})$ controllers using four sensors (z_1, z_2, z_3, z_4) with one (g_1), two (g_1, g_3), three (g_1, g_2, g_3) and four actuators.

manufactured solution $y^*(x, t) = y(x, 0)u^*(t)$. Since the solution is not exact, inserting this solution into the PDE results in a residual that does not cancel out. This residual is added as the source term to the right-hand side of the PDE to create a modified PDE for which the artificial solution is correct and can thus be used for comparison. A sinusoidal input is applied $u^*(t) = cos(\pi t)$ and the resulting state-space models are integrated over a time span of 1 second using a low sample time of $\Delta t = 0.001$ to minimise the errors from the time integration. The maximum error of spline solutions of various degrees against the manufactured solution is shown in Figure 6.

$S_d^2(\mathcal{T}_{56})$ state-space models for the original system are used to synthesise the controller (60). The measured output is also chosen as the controlled output and the input weight is set to $R = diag(0.01)$. A high-order $s \in S_9^2(\mathcal{T}_{120})$ model is assumed to represent original DPS and is used to simulate the response. Figure 7 shows the real part of the most dominant eigenvalue of the closed-loop system for various sensor/actuator configurations. We were able to lower the degree to $d = 5$ after which the stabilisation effect is lost at $d = 4$ which is in accordance with the validation results in Figure 6. The $s \in S_6^2(\mathcal{T}_{56})$ model gives a good balance between performance and model order (see Table 3), and is used to implement the controller. Figure 8 shows the dominant eigenvalues of the $s \in S_6^2(\mathcal{T}_{56})$ control model and the $s \in S_9^2(\mathcal{T}_{120})$ simulation model. It can be observed that the eigenvalues of the control and simulation model coincide well and that they only differ significantly in the highly damped region ($Re\ \lambda < -4.5$). As a result, the controller effectively stabilises the system as can be seen in Figure 9. As a final study, we keep the $s \in S_6^2(\mathcal{T}_{56})$ controller but vary the number of observation points used for feedback (Figure 10(a)) and the number of actuators used for control (Figure 10(b)). It can be observed that effective feedback stabilisation can be achieved using a minimal amount of sensors and actuators.

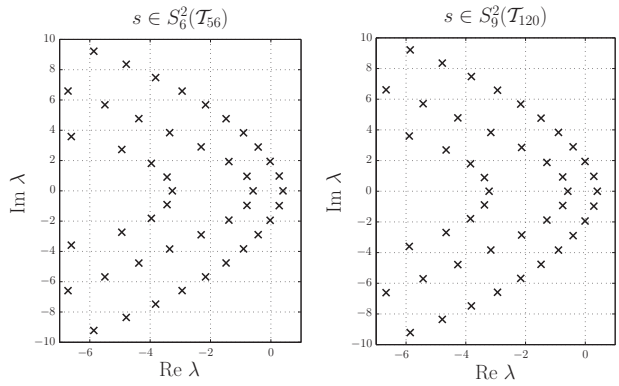

Figure 8. Dominant system poles of the $s \in S_6^2(\mathcal{T}_{56})$ control model (left) and of the $s \in S_9^2(\mathcal{T}_{120})$ simulation model (right).

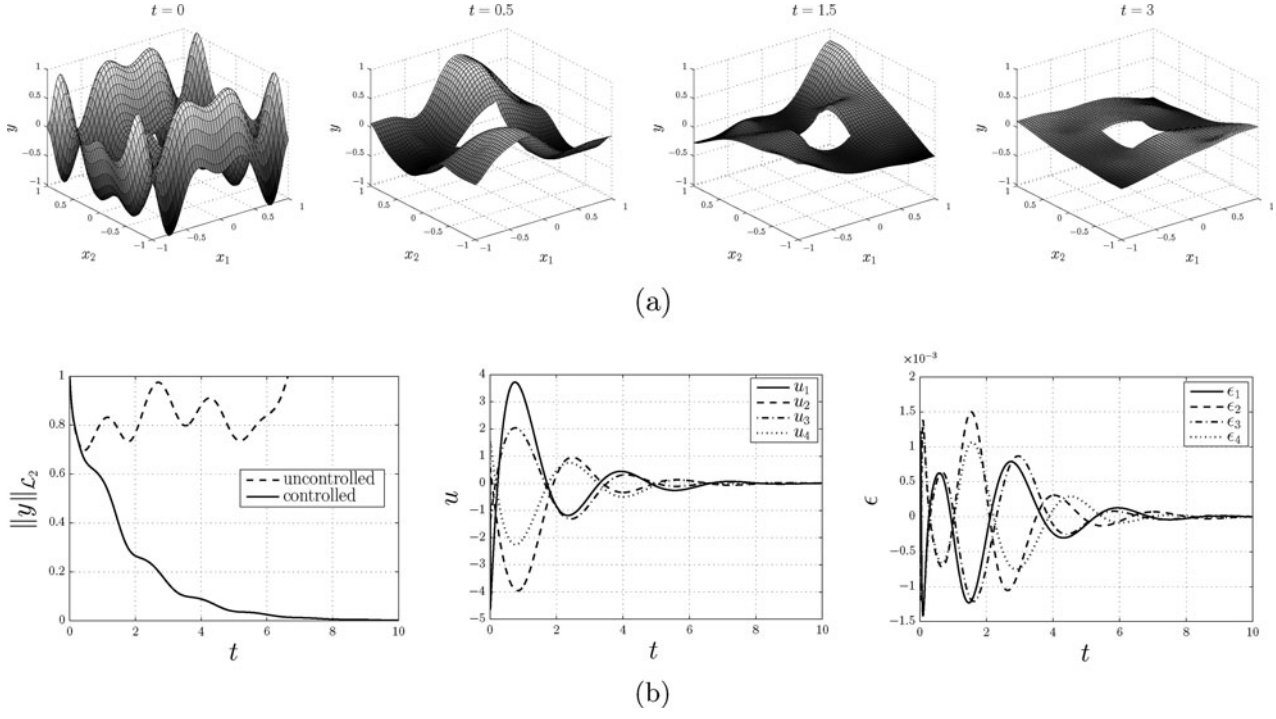

Figure 9. Closed-loop response of the $s \in S_6^2(\mathcal{T}_{56})$ controller using four sensors and four actuators. An $s \in S_9^2(\mathcal{T}_{120})$ Galerkin model is used for simulating the response. (a) Response at four time instants, (b) $\mathcal{L}_2$ norm (left), control inputs (middle) and observer estimation errors (right).

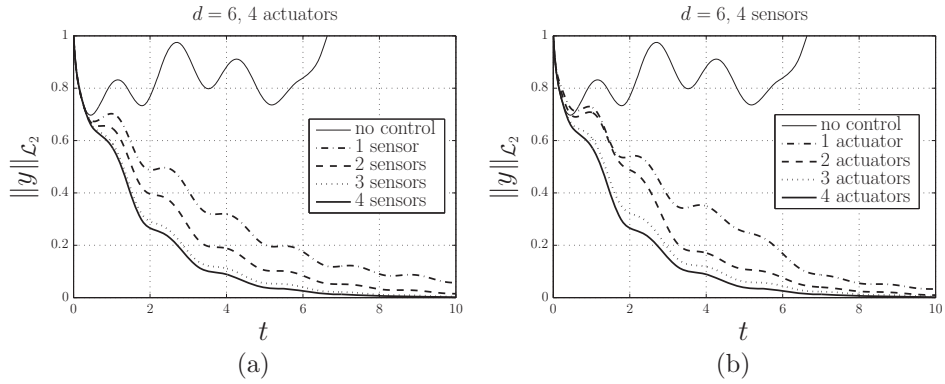

Figure 10. $\mathcal{L}_2$ norm of the state for various controllers. An $s \in S_9^2(\mathcal{T}_{120})$ model is used as the 'true system'. (a): $s \in S_6^2(\mathcal{T}_{56})$ controller using four actuators with one (z_1), two (z_1, z_3), and four sensors. (b): $s \in S_6^2(\mathcal{T}_{56})$ controllers using four sensors with one (g_1), two (g_1, g_3), three (g_1, g_2, g_3) and four actuators.

8. Conclusions

This paper presented a new framework for model reduction of parabolic PDEs on general geometries using multivariate B-splines. The method uses Galerkin projection with B-splines to derive state-space descriptions that can be used for control design. The method can be used to design both in-domain and boundary feedback controllers for PDEs. The effectiveness of the proposed reduction scheme is demonstrated using two examples, a 1-D unstable reaction–diffusion equation and a 2-D unstable reaction–convection–diffusion equation with spatially varying coefficients on an irregular domain. Numerical convergence results show that the proposed reduction scheme results in accurate low-order models of the PDE. The reduced-order models are successfully applied to design and implement feedback controllers for the two test cases. It is shown that effective feedback stabilisation can be achieved using low-order controllers with a minimal amount of state information from sensors.

In this paper, we restricted our attention to a class of linear PDEs. Significant work remains to be done in applying this method to more complex PDE models of chemical processes and fluid flows. Such control problems are often formulated on higher dimensional irregular geometries and are very tractable by the multivariate spline reduction method. Future work will focus on extending this method to coupled and nonlinear PDE systems to further evaluate its effectiveness for practical applications of PDE control.

Disclosure statement

No potential conflict of interest was reported by the authors.

References

Armaou, A., & Christofides, P.D. (2001a). Finite-dimensional control of nonlinear parabolic PDE systems with time-dependent spatial domains using empirical eigenfunctions. *Applied Mathematics and Computer Science, 11*(2), 287–318.

Armaou, A., & Christofides, P.D. (2001b). Robust control of parabolic PDE systems with time-dependent spatial domains. *Automatica, 37*(1), 61–69.

Armaou, A., & Christofides, P.D. (2002). Dynamic optimization of dissipative PDE systems using nonlinear order reduction. *Chemical Engineering Science, 57*(24), 5083–5114.

Awanou, G., & Lai, M.J. (2004). Trivariate spline approximations of 3D Navier–Stokes equations. *Mathematics of Computation, 74*(250), 585–601.

Awanou, G., Lai, M.J., & Wenston, P. (2005). The multivariate spline method for scattered data fitting and numerical solutions of partial differential equations. In G. Chen & M.J. Lai (Eds.), *Wavelets and splines* (pp. 24–75). Brentwood, TN: Nashboro Press.

Baccoli, A., Pisano, A., & Orlov, Y. (2015). Boundary control of coupled reaction-diffusion processes with constant parameters. *Automatica, 54*, 80–90.

Baker, J., Armao, A., & Christofides, P.D. (2000). Finite-dimensional approximation and control of non-linear parabolic PDE systems. *International Journal of Control, 73*(5), 439–456.

Balas, M.J. (1979). Feedback control of linear diffusion processes. *International Journal of Control, 29*(3), 523–534.

Balas, M.J. (1983). The Galerkin method and feedback control of linear distributed parameter systems. *Journal of Mathematical Analysis and Applications, 91*(2), 527–546.

Balas, M.J. (1984). Stability of distributed parameter systems with finite-dimensional controller-compensators using singular perturbations. *Journal of Mathematical Analysis and Applications, 99*(1), 80–108.

Bamieh, B., Paganini, F., & Dahleh, M. (2002). Distributed control of spatially invariant systems. *IEEE Transactions on Automatic Control, 47*(7), 1091–1107.

Christofides, P.D. (2001). *Nonlinear and robust control of PDE systems: Methods and applications to transport-reaction processes*. Springer Science & Business Media. New York, NY.

Christofides, P.D., & Baker, J. (1999). Robust output feedback control of quasi-linear parabolic PDE systems. *Systems and Control Letters, 36*(5), 307–316.

Christofides, P.D., & Daoutidis, P. (1997). Finite-dimensional control of parabolic PDE systems using approximate

inertial manifolds. *Journal of Mathematical Analysis and Applications, 216*(2), 398–420.

Chung, K.C., & Yao, T.H. (1977). On lattices admitting unique lagrange interpolations. *SIAM Journal on Numerical Analysis, 13*(4), 735–743.

Curtain, R.F., & Zwart, H.J. (1995). *An introduction to infinite-dimensional linear systems theory*. New York, NY: Springer-Verlag.

de Boor, C. (1987). B-form basics. In G. Farin (Ed.) *Geometric modeling: Algorithms and new trends* (pp. 131–148). Philadelphia: SIAM Publications.

de Visser, C.C., Chu, Q.P., & Mulder, J.A. (2009). A new approach to linear regression with multivariate splines. *Automatica, 45*(12), 2903–2909.

de Visser, C.C., Chu, Q.P., & Mulder, J.A. (2011). Differential constraints for bounded recursive identification with multivariate splines. *Automatica, 47*(9), 2059–2066.

Farin, G. (1986). Triangular Bernstein-Bézier patches. *Computer Aided Geometric Design, 3*(2), 83–127.

Govindarajan, N., de Visser, C.C., & Krishnakumar, K. (2014). A sparse collocation method for solving time-dependent HJB equations using multivariate B-splines. *Automatica, 50*(9), 2234–2244.

Hagen, G., Mezić, I., & Bamieh, B. (2004). Distributed control design for parabolic evolution equations: Application to compressor stall control. *IEEE Transactions on Automatic Control, 49*(8), 1247–1258.

Hölzel, M.S., & Bernstein, D.S. (2014). A matrix nullspace approach for solving equality-constrained multivariable polynomial least-squares problems. *Automatica, 50*(12), 3030–3037.

Hu, X.L., Han, D.F., & Lai, M.J. (2007). Bivariate splines of various degrees for numerical solution of partial differential equations. *SIAM Journal on Scientific Computing, 29*(3), 1338–1354.

Jovanović, M.R., & Bamieh, B. (2006). A formula for frequency responses of distributed systems with one spatial variable. *Systems & control letters, 55*(1), 27–37.

Lai, M.J., & Schumaker, L.L. (1998). On the approximation power of bivariate splines. *Advances in Computational Mathematics, 9*(3–4), 251–279.

Lai, M.J., & Schumaker, L.L. (2007). *Spline functions on triangulations* (Vol. 110). Cambridge: Cambridge University Press.

Lai, M.J., & Wenston, P. (2004). Bivariate splines for fluid flows. *Computers & Fluids, 33*(8), 1047–1073.

Lasiecka, I., & Triggiani, R. (2000). *Control theory for partial differential equations: Volume 1, Abstract parabolic systems: Continuous and approximation theories* (Vol. 1). Cambridge: Cambridge University Press.

Li, H.X., & Qi, C. (2010). Modeling of distributed parameter systems for applications—a synthesized review from time–space separation. *Journal of Process Control, 20*(8), 891–901.

Roache, P.J. (2002). Code verification by the method of manufactured solutions. *Journal of Fluids Engineering, 124*(1), 4–10.

Rowley, C.W. (2005). Model reduction for fluids, using balanced proper orthogonal decomposition. *International Journal of Bifurcation and Chaos, 15*(03), 997–1013.

Smyshlyaev, A., & Krstic, M. (2004). Closed-form boundary state feedbacks for a class of 1-D partial integro-differential equations. *IEEE Transactions on Automatic Control, 49*, 2185–2201.

Smyshlyaev, A., & Krstic, M. (2005). Backstepping observers for a class of parabolic PDEs. *Systems and Control Letters, 54*(7), 613–625.

Vazquez, R., & Krstic, M. (2007a). A closed-form feedback controller for stabilization of the linearized 2-D Navier–Stokes Poiseuille system. *IEEE Transactions on Automatic Control, 52*(12), 2298–2312.

Vazquez, R., & Krstic, M. (2007b). *Control of turbulent and magnetohydrodynamic channel flows: boundary stabilization and state estimation*. New York, NY: Springer Science & Business Media.

Von Golitschek, M., & Schumaker, L.L. (2002). Bounds on projections onto bivariate polynomial spline spaces with stable local bases. *Constructive Approximation, 18*(2), 241–254.